J Mater Sci (2006) 41:5699–5703
DOI 10.1007/s10853-006-0068-x

LETTER

Self-propagating high-temperature synthesis (SHS) of rotator mixed and mechanically alloyed Ni/Al powder compacts

K. Morsi · S. Shinde · E. A. Olevsky

Received: 10 October 2005 / Accepted: 23 March 2006 / Published online: 16 May 2006

A significant amount of work has been published on the combustion synthesis of nickel aluminides including thermal explosion and SHS type of ignition, [1–4]. In the SHS of nickel aluminides, nickel and aluminum powders are mixed in the desired composition and pressed into a compact, which is then ignited at one end, usually with the aid of a tungsten-heating coil (Fig. 1). An exothermic reaction proceeds converting the nickel and aluminum powders into the desired intermetallic compound, and raises the compact temperature to the maximum *combustion temperature*.

The elemental powders are normally turbula or rotator mixed prior to compaction. On the other hand, recently, mechanical activation of elemental powders prior to SHS (mechanically activated SHS (MASHS)) has also been conducted [5–9]. In MASHS the powders are mechanically alloyed by ball milling under certain conditions that do not give rise to reactions between the elemental powders. In this process nanostructured elemental powders are generated prior to SHS. The process has a number of advantages including the production of a nanostructured product phase; however the resulting product is reported to contain high levels of porosity attributed to entrapped gas during the mechanical alloying process [10]. In the present paper, the concepts of the theory of plasticity of porous bodies are employed to assess the influence of mechanical alloying (MA) on the theoretical yield stress of Ni–Al powder compacts (for nickel particle sizes of 8–15 and 3–7 μm). The effect of MA (low-energy mechanical mixing) on SHS characteristics are reported, together with the influence of degassing-MA-SHS sequential order on resulting product porosity, which may possibly have implications for MASHS in general. Powders of nickel (Novamet Inc., USA) and aluminum (−325 mesh, average particle size ~11 μm, Atlantic Engineers, USA), were mixed in the composition of Ni_3Al. Two sample compositions were produced, each with a different nickel particle size (3–7 and 8–15 μm, respectively). For each composition, mixing was conducted over two stages. First, the powders were gently mixed for 1.5 h using a powder rotator mixer. Second, approximately 5–6 g of Ni/Al powders were separately mechanically alloyed (low-energy mechanically mixed) in hardened steel vials, using twenty tungsten carbide balls (diameter 3 mm) at 240 rpm for 27 h. Specimens that have just been mixed using the powder rotator without MA are referred to in this paper as have undergone rotator mixing. Powders that were rotator mixed followed by MA for 27 h are referred to as MA 27 h. Each powder was then uniaxially pressed into rectangular specimens of dimensions shown in (Fig. 1). Zinc stearate lubricant was mixed in acetone and applied to the inner walls of the hardened steel compaction die used. All powder compacts were vacuum degassed at 150 °C for 10.5 h. A K-type thermocouple was inserted at half height into the specimen to monitor the temperature–time profile during the reaction. Specimens were then reacted in an SHS reactor under an argon atmosphere (three specimens were used for each particle size and mixing sequence, and average combustion temperatures were then reported). The top of the specimens were placed at a distance approximately 2–3 mm beneath the tungsten coil, which was subsequently subjected to 750 W. Each powder mixture (mechanically alloyed and

K. Morsi (✉) · S. Shinde · E. A. Olevsky
Department of Mechanical Engineering, San Diego State University, 5500 Campanile Drive, San Diego, California 92182, USA
e-mail: kmorsi@mail.sdsu.edu

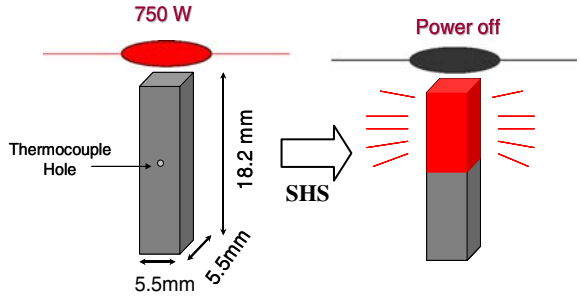

Fig. 1 Schematic of SHS experimental setup

rotator mixed) was also separately uniaxially pressed into discs of diameter 8 mm and height 2–3 mm at four different compaction pressures (three specimens were compacted at each pressure and results averaged), to analyze its compaction behavior and calculate the compact yield strength. The density of green specimens was determined by weighing and measuring the specimen dimensions using digital micrometers and calipers. The porosity content of the reacted specimens was determined using image analysis. For microstructural characterization, reacted samples were cut centrally along their length, ground and polished to 1 μm diamond finish, with ultrasonic cleaning between polishing stages. Light and scanning electron microscopy (secondary electron and backscattered, Hitachi S-2700 & Amray 1830 I) were used to characterize the microstructure and determine the phase distribution. The theoretical yield stresses of the compacts were calculated by combining experimental compaction results and theory. The yield surface of a rigid-plastic porous material is given by Eq. (1) [11]:

$$\frac{p^2}{\psi}+\frac{\tau^2}{\varphi}=\sigma_y^2(1-\theta) \tag{1}$$

where σ_y is the yield limit of a fully dense material (theoretical yield stress), ψ and ϕ are the bulk and shear moduli of the porous material, θ is the porosity (θ = 1–ρ, where ρ is the relative density), p and τ are the first invariant of the stress tensor and the second invariant of the stress tensor deviator, respectively.

For pressing in a rigid die, Eq. (1) leads to the following expression which interrelates the axial stress σ_z, theoretical yield stress σ_y, and porosity θ:

$$\sigma_z=\frac{2}{3}\sigma_y\frac{(1-\theta)^{3/2}}{\sqrt{\theta}} \tag{2}$$

In the derivation of Eq. (2) friction at the die walls is neglected and for the bulk ψ and shear ϕ moduli of the porous material the following model [11–13] is employed:

$$\psi=\frac{2}{3}\frac{(1-\theta)^3}{\theta};\ \varphi=(1-\theta)^2 \tag{3}$$

Equation (2) was used as the basis for the analytical approximation of the experimental data represented in Table 1 (spring back effects where calculated and found to be insignificant). The corresponding inverse regression analysis enabled the determination of the theoretical yield stress before and after mechanical alloying for both particle sizes.

Table 1 is a summary of results obtained. It is clear that for both rotator mixed and MA powders, the compact theoretical yield stress increases with a decrease in Ni particle size. This is due to the corresponding decrease in the average compact particle size.

The higher theoretical yield stress for the MA 27 h samples compared to their rotator mixed counterparts for both Ni particle size samples (3–7 and 8–15 μm) is due to work hardening and a possible slight reduction in average particle size especially for the 8–15 μm Ni samples. Scanning electron micrographs of all powders used are shown in Fig. 2.

A typical temperature–time profile is shown in (Fig. 3) for the rotator-mixed Ni (8–15 μm)/Al powder compact. Ignition is seen to occur at a temperature of ~400 °C, i.e. the specimen at this point was preheated to this temperature before the reaction wave had arrived. In fact without preheating, it would not have been possible to obtain a self-sustaining reaction for Ni_3Al. The ignition temperature was approximately the same for all specimens investigated, and the temperature–time profile did not significantly change from one specimen to the other. A major requirement for successful processing is that the aluminum (the lower melting point phase) be continuous around the nickel particles throughout the microstructure prior to the reaction [4, 14] to facilitate the spreading of molten Al during the reaction. Normally this is achieved by careful selection of

Table 1 Summary of compact theoretical yield stress and combustion temperature

Nickel particle size (μm)	Compact theoretical yield stress (MPa)		Average combustion temperature (°C)	
	Rotator mixed	MA 27 h	Rotator mixed	MA 27 h
3–7	220	233	1240	1203
8–15	195	213	1154	1195

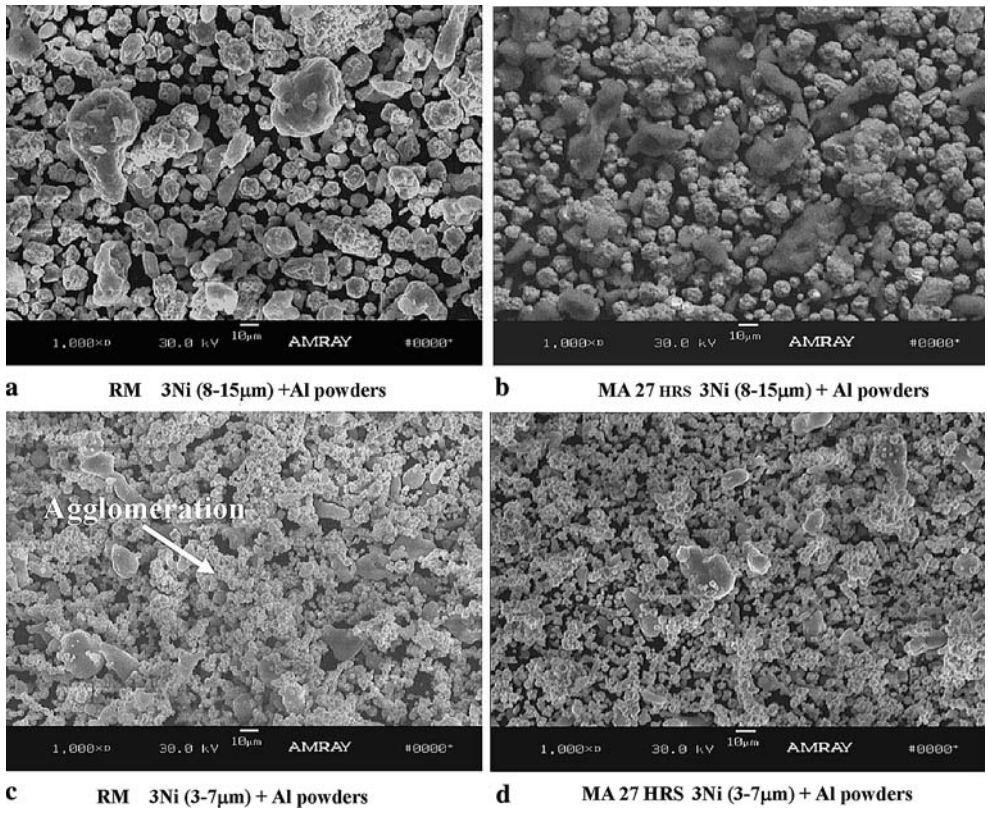

Fig. 2 Effect of mechanical alloying on morphology and distribution of nickel and aluminum powders. Break up of agglomerates is shown for the 3–7 μm Ni sample following MA (**c** and **d**)

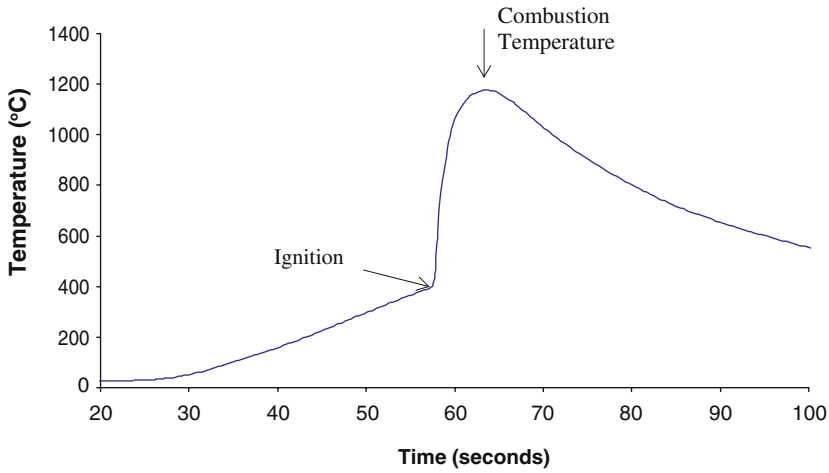

Fig. 3 Temperature–time profile during SHS of Ni (8–15 μm)–Al powder compact

the particle size ratio of the two elemental powders (i.e. Ni particle size would need to be ~2.4 greater than Al for the Ni_3Al composition to ensure continuous Al phase in accordance with percolation theory). Nickel at the 3–7 μm particle size has been known to agglomerate to sizes ~45 μm in diameter [4], which when mixed with Al of the particle size presently used, can generate an interconnected network of Al in the green compact prior to the reaction. The interconnection of Al is expected however to be hindered if the 8–15 μm Ni is used (which have minimal agglomeration), possibly giving rise to inefficient reaction characteristics. The decrease in combustion temperature for the 3–7 μm after MA could be a result of some Ni agglomerate break down (as seen in Fig 2c, d) and hence some possible loss of Al interconnectivity. XRD analysis on the reacted specimens revealed that they all consisted of a multiphase microstructure including Ni_3Al (major phase), unreacted Ni & Al, Al_3Ni_2 and Al_3Ni_5. Therefore the reaction did not go to completion for all specimens investigated rotator mixed and mechanical alloyed. It appears that under the current low-energy milling conditions mechanical activation was not achieved, in the way

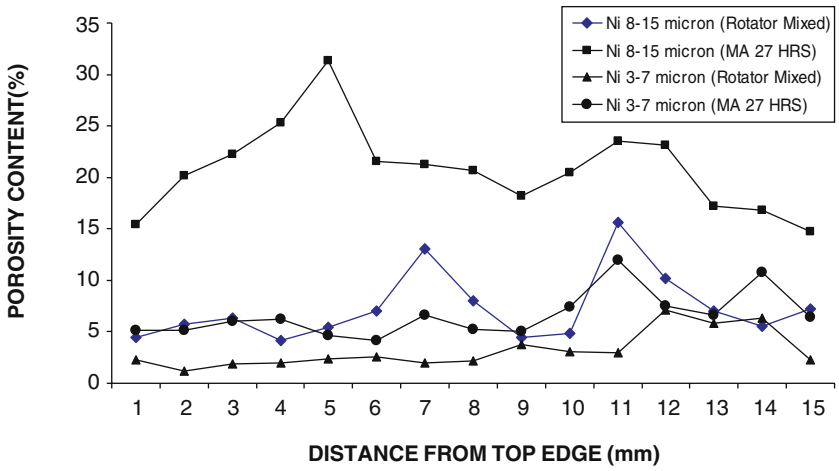

Fig. 4 Porosity profile along the central line of reacted rectangular specimens from top (i.e. near the tungsten coil) to bottom for all investigated Ni/Al powder compacts

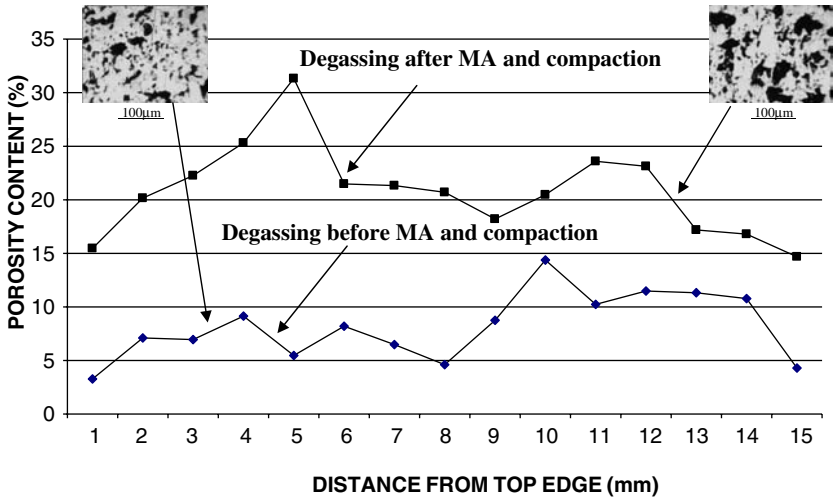

Fig. 5 Effect of powder degassing on porosity profile along the central line of reacted green compacts of 3Ni–Al powders (8–15 µm Ni) 27 h MA

typically known for MASHS, which is usually conducted under more aggressive milling conditions.

The porosity profile along the central line of reacted rectangular specimens from top (i.e. near the tungsten coil) to bottom is shown in (Fig. 4). It can be seen that MA tends to result in an increase in the level of SHS product porosity, this is especially apparent for the 8–15 µm Ni compacts. One of the possible reasons for porosity generation in SHS is the presence of adsorbed water or low boiling point impurities on the surface of powders prior to SHS. During SHS the expansion of gasses can result in increased porosity. It is not known why this is more apparent in the 8–15 µm Ni than the 3–7 µm. The degassing stage in this paper was carried out on the green compacts (which were previously pressed to ~74–76% theoretical density). At this density, the majority of pores are expected to be interconnected which should facilitate degassing. However, we also carried out the exact experiment for the 8–15 µm Ni but instead of degassing the green compacts, we degassed the as-received powders, prior to MA. The results are compared for the 8–15 µm Ni in (Fig. 5), showing that degassing-MA-SHS sequence can have a significant effect on product porosity content. The porosity is considerably reduced by simply degassing the powders prior to MA. These findings may have significant implications for processes such as MASHS.

References

1. Biswas A, Roy SK, Gurumurthy KR, Prabhu N, Banerjee S (2002) Acta Materialia 50(4):757
2. Yeh LC, Sung YW (2004) J Alloys Compd 384(1–2):181
3. Philpot KA, Munir ZA, Holt JB (1987) J Mater Sci 22(1):159
4. Misiolek W, German RM (1991) Mater Sci Eng A-Struct Mater Prop Microstruct Process 144(1–2):1
5. Eric Gaffet, Frederic Bernard (2002) Ann Chim Sci Mat 27(6):47

6. Gauthier V, Bernard F, Gaffet E, Josse C, Larpin PJ (1999) Mater Sci Eng A-Struct Mater Prop Microstruct Process 272(2):334
7. Gauthier V, Bernard F, Gaffet E, Vrel D, Gailhanou M, Larpin PJ (2002) Intermetallics 10(4):377
8. Gauthier V, Josse C, Bernard F, Gaffet E, Larpin PJ (1999) Mater Sci Eng A-Struct Mater Prop Microstruct Process 265(1–2):117
9. Anselmi Tamburini U, Maglia F, Spinolo G, Doppiu S, Monagheddu M, Cocco G (2000). J Mater Synth and Process 8(5–6):377
10. Eric gaffet, Frederic Bernard (2002) Ann Chim Sci Mat 27(6):47
11. Olevsky E (1998) Mater Sci Eng R Rev 23(2):41
12. Green RG (1972). Int J Mech Sci 4:109
13. Shtern BM (1982) Phenomenological theories of pressing of powders, Naukova Dumka, Kiev
14. Morsi K (2001) Mater Sci Eng A A299:1